THE GEOLOGICAL SOCIETY OF AMERICA®

# Rates of bedrock canyon incision by megafloods, Channeled Scabland, eastern Washington, USA

**Karin E. Lehnigk[1,†,*], Isaac J. Larsen[1], Michael P. Lamb[2], and Scott R. David[1,*]**
[1]*Department of Earth, Geographic, and Climate Sciences, University of Massachusetts, 233 Morrill Science Center, 627 North Pleasant Street, Amherst, Massachusetts 01003-9297, USA*
[2]*Division of Geological and Planetary Sciences, California Institute of Technology Mail Code 170-25, 1200 E. California Boulevard, Pasadena, California 91125, USA*

## ABSTRACT

**Pleistocene outburst floods from the drainage of glacial Lake Missoula carved bedrock canyons into the Columbia Plateau in eastern Washington, USA, forming the Channeled Scabland. However, rates of bedrock incision by outburst floods are largely unconstrained, which hinders the ability to link flood hydrology with landscape evolution in the Channeled Scabland and other flood-carved landscapes. We used long profiles of hanging tributaries to reconstruct the pre-flood topography of the two largest Channeled Scabland canyons, upper Grand Coulee and Moses Coulee, and a smaller flood-eroded channel, Wilson Creek. The topographic reconstruction indicates floods eroded 67.8 km$^3$, 14.5 km$^3$, and 1.6 km$^3$ of rock from upper Grand Coulee, Moses Coulee, and Wilson Creek, respectively, which corresponds to an average incision depth of 169 m, 56 m, and 10 m in each flood route. We simulated flood discharge over the reconstructed, pre-flood topography and found that high-water evidence was emplaced in each of these channels by flow discharges of $3.1 \times 10^6$ m$^3$ s$^{-1}$, $0.65–0.9 \times 10^6$ m$^3$ s$^{-1}$, and $0.65–0.9 \times 10^6$ m$^3$ s$^{-1}$, respectively. These discharges are a fraction of those predicted under the assumption that post-flood topography was filled to high-water marks for Grand and Moses Coulees. However, both methods yield similar results for Wilson Creek, where there was less erosion. Sediment transport rates based on these discharges imply that the largest canyons could have formed in only about six or fewer floods, based on the time required to transport the eroded rock from each canyon, with associated rates of knickpoint propagation on the order of several km per day. Overall, our results indicate that a small number of outburst floods, with discharges much lower than commonly assumed, can cause extensive erosion and canyon formation in fractured bedrock.**

## INTRODUCTION

Reconstructing the paleodischarge of large floods is important for understanding landscape evolution and mechanisms of abrupt climate change on Earth (Clarke et al., 2004; Praetorius et al., 2020) and Mars (Baker et al., 1991). Outburst floods are capable of eroding deep canyons, particularly in landscapes with fractured bedrock (Bretz, 1923; Baker, 1978c; O'Connor, 1993; Baker and Kale, 1998; Lamb et al., 2014; Baynes et al., 2015b). However, with the exception of limited historical cases where the hydrology and hydraulics of canyon formation and flood erosion are constrained (e.g., Lamb and Fonstad, 2010; Anton et al., 2015; Cook et al., 2018; Bender, 2022), it remains a challenge to understand the rates of landscape evolution generated by repeated outburst floods. Reconstruction of pre-flood topography is necessary to both quantify the volume of bedrock eroded by floods and to interpret paleo-flood discharge from high-water evidence (Larsen and Lamb, 2016; David et al., 2022; Lehnigk and Larsen, 2022). However, without observations of the pre-flood land surface, it can be challenging to reconstruct the topography first encountered by outburst floods. Developing a better understanding of the links between flood hydraulics and the topographic expression of outburst flood erosion can aid in assessing paleo-flood discharge from topographic data alone, which is particularly relevant for interpreting the history of water on Mars, where canyon geometry provides one of the few observable constraints on paleo-flood discharge (e.g., Baker, 1982; Lapotre et al., 2016).

The Channeled Scabland in eastern Washington, USA, is an iconic outburst flood-carved landscape (Bretz, 1923). The Channeled Scabland contains several large canyons incised by headward waterfall or cataract (a cataract is a waterfall with high discharge) retreat during Pleistocene outburst floods from glacial Lake Missoula, as well as flood channels that were eroded, but did not evolve into deep canyons (Bretz et al., 1956; Bretz, 1969). Stratigraphic evidence from fine-grained slackwater deposits (Bretz, 1969; Atwater, 1984; Waitt, 1985, 2002) and marine records (Gombiner et al., 2016) have been interpreted to indicate that there were at least dozens of floods. The total number of floods inferred from glacial Lake Missoula by combining evidence from different sites is 104–108, though the incompleteness of the individual records indicates there were likely more (O'Connor et al., 2020). However, many of these floods occurred after canyons were incised into the Columbia Plateau (Baker and Bunker, 1985; Atwater, 1986). Hence, it is unclear how many of the ~100 floods exceeded thresholds for plucking erosion and contributed to landscape evolution.

The routes that outburst floods took across the Columbia Plateau were influenced by pre-existing topography. For instance, floods deepened pre-existing valleys, which generated hanging tributaries that are still graded to the pre-flood base-level (Bretz, 1932; Hanson, 1970; Waitt, 2021). Previous work in a variety of landscapes has shown that extension of hanging tributary long profiles can be used to reconstruct pre-incision topography and thereby estimate the volume of eroded bedrock (Brocklehurst and

Karin E. Lehnigk https://orcid.org/0000-0001-7239-3913
†klehnigk@gmail.com
*Present address: Karin E. Lehnigk, Department of Earth and Atmospheric Sciences, Georgia Institute of Technology, 311 Ferst Drive, Atlanta, Georgia 30318, USA; Scott R. David, Department of Watershed Sciences, Utah State University, 5210 Old Main Hill, Logan, Utah 84322-5210, USA

*GSA Bulletin*; September/October 2024; v. 136; no. 9/10; p. 4398–4410; https://doi.org/10.1130/B36975.1.
Published online 5 April 2024



For permission to copy, contact editing@geosociety.org
© 2024 Geological Society of America

Downloaded from http://pubs.geoscienceworld.org/gsa/gsabulletin/article-pdf/136/9-10/4398/6900623/b36975.1.pdf?casa_token=IUGEppbvuJUAAAAA:cP-Iqvj09IGdMOx5aYgrxkIN0Y9yBKjypGEIlcxz3I4RsuNXqhxJW7HKJC
by Univ of Massachusetts Amherst user

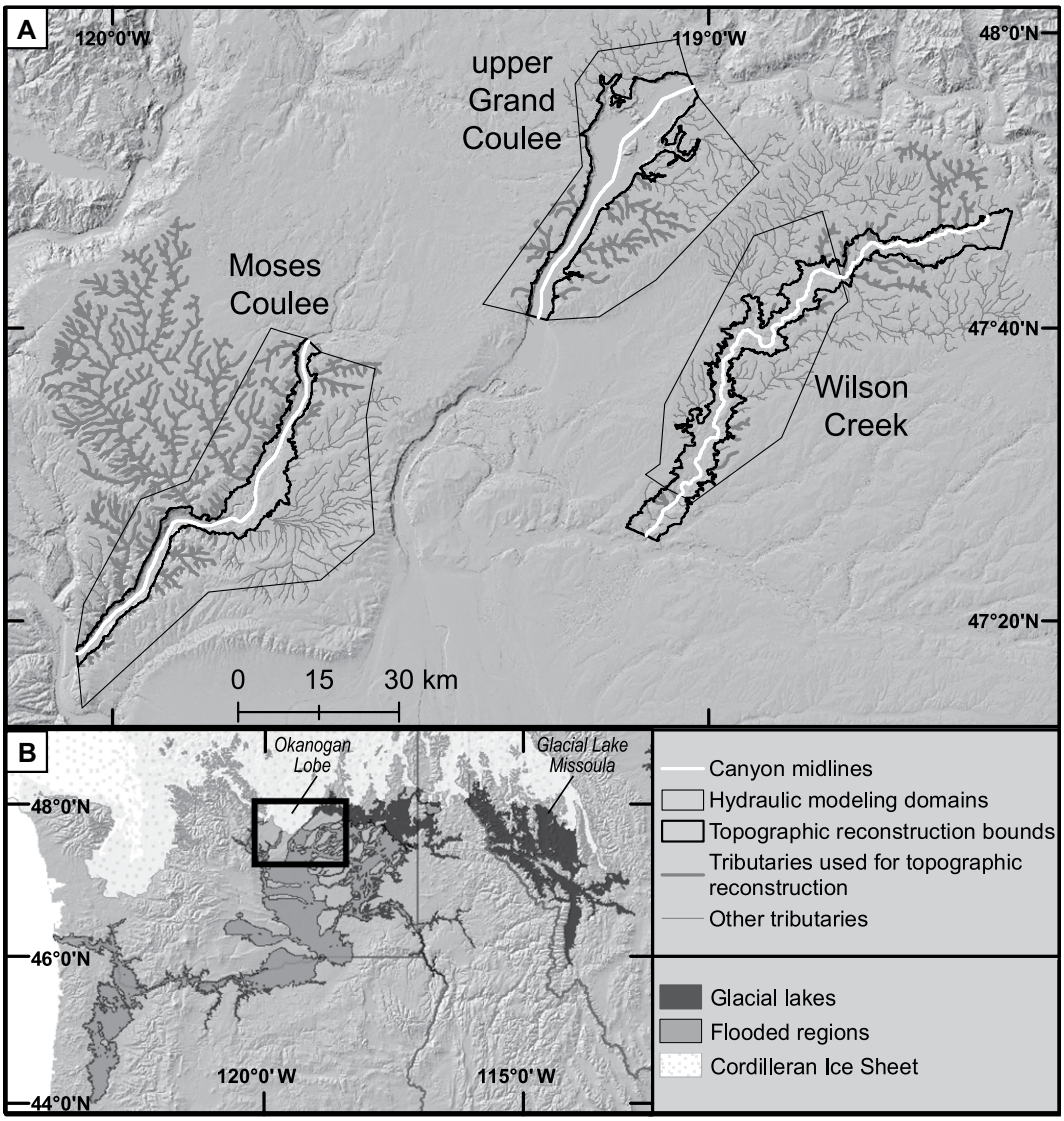


**Figure 1. (A) The study area showing locations of the three flood channels (upper Grand Coulee, Moses Coulee, and Wilson Creek) where we reconstructed topography and flood discharges. (B) The location of the study area in the northwestern USA showing the locations of ice lobes, glacial lakes, and areas inundated by floods from glacial Lake Missoula during the last glaciation (Ehlers et al., 2011).**

Whipple, 2006; Valla et al., 2010; Fox, 2019), including efforts by Hanson (1970) to manually reconstruct paleo-tributary profiles and approximate the pre-flood paleo-topography of Moses Coulee in the Channeled Scabland. In this study, we build on the work of Hanson (1970) and use quantitative slope-distance relationships from bedrock streams to reconstruct pre-flood stream networks and topographic surfaces. By comparing the reconstructed topography against the present-day topography, we quantify the volume of rock eroded from three sites: Grand Coulee and Moses Coulee, the two largest flood-carved canyons in the Channeled Scabland, and Wilson Creek—a smaller channel that was eroded by floods but did not develop a large knickpoint or deep canyon topography. We then use hydraulic models to constrain the paleo-discharge that matches high-water evidence on the pre-incision topography and use modeled shear stresses to predict sediment flux, erosion and knickpoint retreat rates, and the number of floods required to erode each canyon or flood channel.

## STUDY SITE

The Channeled Scabland (Fig. 1) is a landscape of fluvially scoured bedrock formed by outburst floods from glacial Lake Missoula (Pardee, 1942; Bretz et al., 1956). During the last glaciation, floods from glacial Lake Missoula overtopped the Columbia and Spokane River valleys and flowed across a broad plateau formed by the Miocene-age Columbia River flood basalt (Barry et al., 2013). As floods crossed the Columbia Plateau, they eroded the columnar and jointed bedrock primarily by plucking (Bretz, 1923, 1928b, 1969; Bretz et al., 1956; Baker, 1973; Lapotre et al., 2016; Larsen and Lamb, 2016; Lehnigk and Larsen, 2022). In the northwest portion of the Channeled Scabland, cataract retreat driven by floods spilling out of the Columbia valley into pre-existing drainage networks carved upper Grand Coulee and Moses Coulee, the two largest canyons in the Channeled Scabland. Floodwater overtopped drainage divides at 660–720 m and 655–710 m (Waitt, 2021) to form canyons with depths up to 240 m and 220 m and lengths of 37 km and 56 km in upper Grand Coulee and Moses Coulee, respectively. Floods also eroded the Wilson Creek drainage, spilling over drainage divides at higher elevations of 708–730 m (Waitt, 2021) to form a narrower 90-km-long channel with a maximum valley depth of ~80 m.

Flood pathways and associated erosion in the channels shifted during the course of flooding from glacial Lake Missoula in response to changing ice margins and topography (Balbas et al., 2017; O'Connor et al., 2020; Denlinger



Downloaded from http://pubs.geoscienceworld.org/gsa/gsabulletin/article-pdf/136/9-10/4398/6900623/b36975.1.pdf?casa_token=IUGEppbvuJUAAAAA:cP-Iqvj09IGdMOx5aYgrxkIN0Y9yBKjypGEIlcxz3I4RsuNXqhxJW7HKJC
by Univ of Massachusetts Amherst user

et al., 2021; Pico et al., 2022). The timing of the origin of Grand Coulee is debated (Waitt et al., 2021). Bretz (1932) speculated that flooding during multiple glaciations may have been required to erode Grand Coulee and interpretation of stratigraphy has led to the conclusion that incision of Grand Coulee was completed before the end of the last glaciation, and potentially during a prior glaciation (Atwater, 1986). However, more recent geochronology and hydraulic modeling results indicate the incision of upper Grand Coulee was more likely completed during the late Pleistocene, after ca. 18 ka (Balbas et al., 2017; O'Connor et al., 2020; Denlinger et al., 2021; Waitt et al., 2021).

The maximum extent of flood inundation is constrained by depositional and erosional features, which are called "high-water marks." Examples of high-water marks that record minimum flood stage include ice-rafted erratics inferred to have been deposited in shallow water at flow margins, erosional scarps in the loess that covers the uplands of the Columbia Plateau, or the highest drainage divides overtopped by floods (e.g., Baker, 1978a). However, using these high-water marks to constrain flood sizes is challenging due to uncertainty in the elevation of the pre-incision valley floor at the time of emplacement (Larsen and Lamb, 2016; Lehnigk and Larsen, 2022).

Locations of focused bedrock incision in the Channeled Scabland are predominantly associated with geological structures that fractured rock and generated topographic relief. The cataract that retreated through upper Grand Coulee initiated at the Coulee monocline (Bretz, 1932) and the most extensive erosion in Moses Coulee occurred where floods crossed the Badger Mountain anticline (Fig. S1[1]); there is >100 m of relief in the landscape associated with each of these structures. In contrast, although folds cross Wilson Creek (Washington State Department of Natural Resources, 2010), none generate substantial relief. With the exception of flood-generated incision, the post-eruption surface of the Columbia Plateau has been thought to be largely preserved (Swanson and Wright, 1978), an inference supported by cosmogenic nuclide concentrations in basalt that indicate the plateau surface has eroded at a rate of only 1.5 m $Ma^{-1}$ since the Miocene (Larsen et al., 2021). Pre-flood drainage routes are thus assumed to have been graded to local baselevels (Bretz, 1932; Hanson, 1970).

There are no field-based estimates of the number of floods that incised upper Grand Coulee, although Bretz (1932, p. 82) hypothesized that the ice of the Okanogan Lobe would only have been sufficiently thick to divert water from the Columbia River into Grand Coulee for long enough to allow about six floods, with possible additional floods during prior glaciations. At least four separate floods have been inferred from upward-fining deposits of basalt clasts at Rock Island Bar at the mouth of Moses Coulee (Waitt, 1985). Gravel beds displaying giant ripples at three distinct elevations that are separated by erosional scarps at the junction of Wilson Creek and Crab Creek have been used to infer that three distinct floods occurred in Wilson Creek (Bretz et al., 1956, p. 980; Bretz, 1969, p. 528). Whereas the geologic record at the mouth of Moses Coulee provides definitive evidence for the minimum number of floods (Waitt, 1985), the flood numbers Bretz proposed for Grand Coulee and Wilson Creek are very speculative, as stratigraphic evidence for multiple floods is lacking at these sites.

## METHODS

### Topographic Reconstruction

We reconstructed topography for upper Grand Coulee, Moses Coulee, and Wilson Creek and tested the reconstruction method on Douglas Creek, a large tributary of Moses Coulee that was not eroded by floods. Pre-flood topography can be inferred by interpolating between the rims of flood eroded canyons (e.g., Baynes et al., 2015a; Larsen and Lamb, 2016; Lehnigk and Larsen, 2022), but such an approach does not account for pre-flood fluvial incision if there was a drainage network prior to flooding, and hence could overestimate elevation. Our topographic reconstruction is based on the observation that in an equilibrium fluvial landscape, as the Channeled Scabland region likely was prior to flooding (Bretz, 1932; Hanson, 1970; Larsen et al., 2021), tributary streams join trunk channels without a break in elevation or slope at junctions (Playfair, 1802; Whipple and Tucker, 1999). As discharge increases with drainage area, channel bed slopes decrease, resulting in a concave-up elevation profile that can be modeled as a power law relationship between local channel slope ($S$, m $m^{-1}$) and drainage area ($A$, $m^2$) as $S = k_s A^{-\theta}$, where $k_s$ ($m^{-2}$) is the steepness index and $\theta$ is a dimensionless concavity index (Hack, 1957; Flint, 1974; Howard and Kerby, 1983). An equilibrium stream has a uniform incision rate (Wobus et al., 2006), which depends on channel bed slope and discharge (Leopold et al., 1964; Howard and Kerby, 1983; Seidl and Dietrich, 1992). Because discharge is proportional to distance from the channel head (Leopold et al., 1964; Hack, 1973), slope can be defined in terms of distance downstream ($L$, m) rather than drainage area as:

$$S = kL^{-\lambda}, \quad (1)$$

where $k$ and $\lambda$ represent a length-dependent steepness index ($m^{-1}$) and dimensionless concavity index, respectively (Bishop and Goldrick, 2000; Goldrick and Bishop, 2007). Using the distance-slope form to describe channel profiles allows a stream profile to be extended beyond the rim of a canyon along its average heading, to intersect with the pre-canyon paleo-valley (Fig. 2).

We identified tributaries lacking evidence of direct impacts from glacial ice or outburst flood erosion and used these to reconstruct pre-incisional topography. Tributaries draining into each canyon or channel were identified on a 10 m digital elevation model (DEM) constructed from U.S. Geological Survey topographic maps with sinks filled (see the Supplemental Material), using a D8 flow algorithm and assuming a threshold drainage area of 1 $km^2$ for channel heads (Montgomery and Dietrich, 1989; Wobus et al., 2006). The profile of the longest reach for each tributary was extracted from the DEM using TopoToolbox (Schwanghart and Scherler, 2014). We identified 48 tributaries draining into upper Grand Coulee, 94 tributaries draining into Moses Coulee, and 69 tributaries draining into Wilson Creek. However, we excluded tributaries from the analysis if mapping (Bretz, 1932; Washington State Department of Natural Resources, 2010; Fig. S1) indicated they were located entirely in areas that were modified by outburst floods or by the Cordilleran ice sheet, or if the resulting extrapolation did not produce a profile that resembled that of a graded stream. The 211 tributaries for which elevation profiles were extracted yielded 17, 65, and 31 tributary elevation profiles that were included in the analysis for upper Grand Coulee, Moses Coulee, and Wilson Creek, respectively (Fig. 1). More details on the justification for the selection of individual tributaries can be found in the Supplemental Material (Tables S1–S3).

The long profiles for each tributary were smoothed to remove noise and eliminate DEM artifacts (e.g., Wobus et al., 2006) using a moving average over a 50 m length scale, a distance 10 times greater than the mean channel width of 5 m that was measured using 1 m resolution aerial imagery (USDA-NRCS-NCGC, 2009). Elevation and distance data extracted from DEM

[1]Supplemental Material. Details about sensitivity testing and validation of the topographic reconstruction methods described in the main text, additional details about modeling methods, and figures and tables with additional details about the study area and models presented in the main text. Please visit https://doi.org/10.1130/GSAB.S.25320616 to access the supplemental material, and contact editing@geosociety.org with any questions.



Downloaded from http://pubs.geoscienceworld.org/gsa/gsabulletin/article-pdf/136/9-10/4398/6900623/b36975.1.pdf?casa_token=IUGEppbvuJUAAAAA:cP-Iqvj09IGdMOx5aYgrxkIN0Y9yBKjypGEIlcxz3I4RsuNXqhxJW7HKJC
by Univ of Massachusetts Amherst user

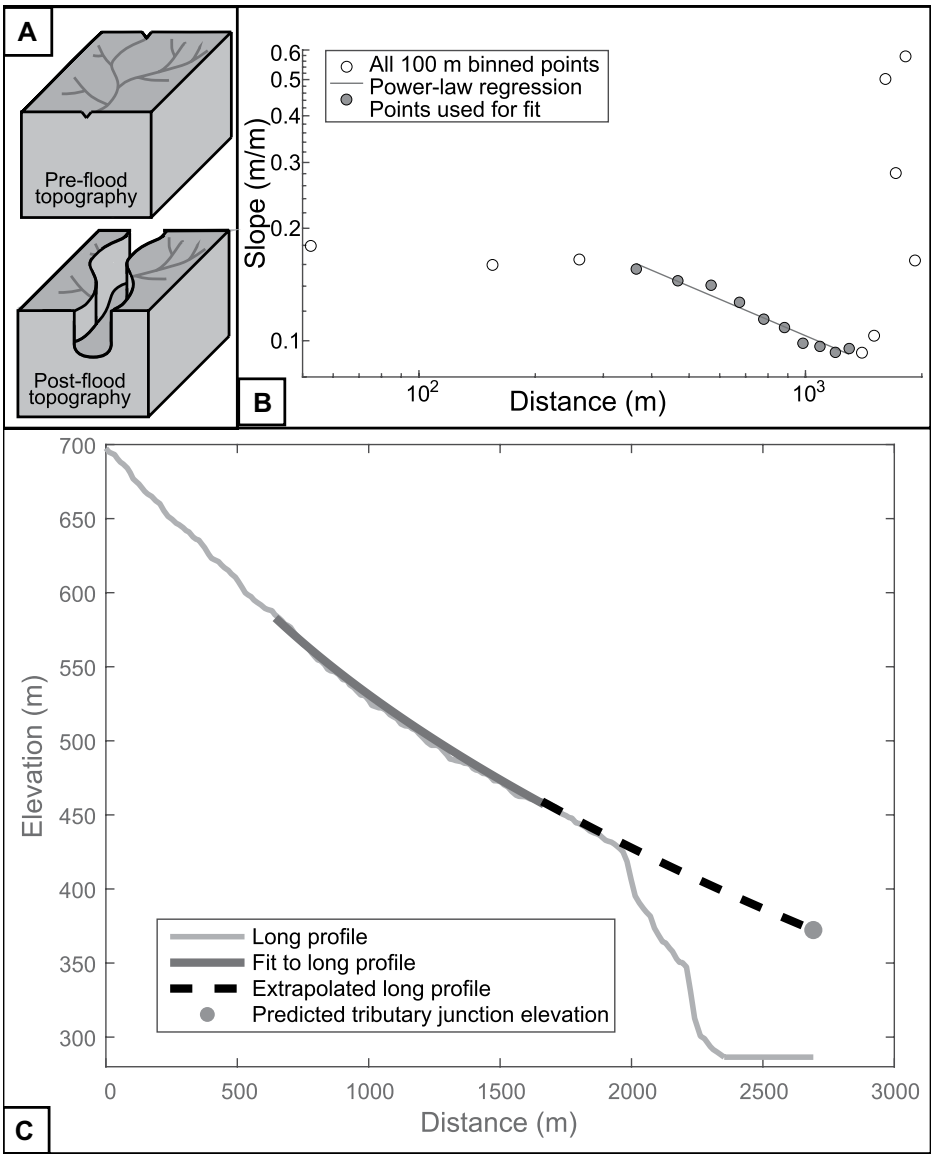


**Figure 2. (A) Schematic illustration of the tributary extrapolation method used to reconstruct pre-flood long profiles. (B) A power-law regression (gray line) was fit through the binned slope-distance points for the tributary reach upstream of the intersection of the canyon rim. (C) The fit was used to extend the tributary elevation-distance profile (solid dark gray line) to the canyon midline (dashed line), producing a new estimate of elevation at the confluence (circle) that was used to reconstruct the pre-flood trunk channel long profile (Fig. 3).**

grid cells along each tributary long profile were binned into 100 m distance increments, and an average slope for each bin was calculated. We assessed the sensitivity to bin width using a range of values and found that the results did not vary (details provided in the Supplemental Material). We manually selected the reach of each tributary that was used to extrapolate slope-distance relationships to use only the portion of the profile adjusted to the pre-flood base-level to exclude short channel segments directly adjacent to the canyon rim where limited enhanced incision in response to flood-induced base-level fall has occurred in some tributaries. The values of $k$ and $\lambda$ in Equation 1 were determined by linear regression through the log-slope log-distance data, using the y-intercept of the regression line as $k$ and the slope as $\lambda$ (Wobus et al., 2006). The sinuosity of each tributary was also calculated as the ratio of the along-channel distance to straight-line distance. Slope and elevation were extrapolated at 10 m intervals as $z_i = z_{i-1} - S_i(x_i - x_{i-1})$, where $S_i$ (m m$^{-1}$) is the slope calculated from Equation 1 at distance $x_i$ (m), yielding a new elevation value $z_i$ (m) at each point (Fig. 2). Extrapolation was completed over the straight-line distance between the point where the tributary stream crossed the canyon rim and the canyon midline along the tributary's average heading, multiplied by the measured sinuosity to account for additional along-channel distance. We identified the intersection of each tributary with the canyon rim manually based on slope-distance data, as slope values increase abruptly downstream from the canyon rim (Fig. 2B). The average stream heading was calculated over 500 m or the distance to the first tributary confluence upstream from the canyon rim, whichever was shorter. We determined the position of the midline for Wilson Creek using the stream network extracted from the DEM, whereas we delineated the midlines of upper Grand Coulee and Moses Coulee manually as a line approximately equidistant between the two canyon rims, as their floors are too flat for a streamflow path to be determined from DEM data. Automated methods for delineating valley midlines exist (Clubb et al., 2022), but we opted for a manual method as adjustments to an automated approach would have been necessary to ensure the delineated midline did not cross large rock monoliths that are present within in the canyons, such as Steamboat Rock in upper Grand Coulee.

To create the reconstructed paleo-long profile of each of the three trunk streams, the confluence elevations of the reconstructed tributary reaches were plotted as a function of distance along the midline of each canyon or flood channel. The maximum elevation of Steamboat Rock, 716 m, was also plotted along the midline of upper Grand Coulee, because its surface was not substantially lowered by flood erosion (Bretz, 1932). A pre-incision longitudinal profile for the trunk channel (Fig. 3) was generated at 10 m resolution for each canyon or channel by smoothing the extrapolated confluence elevations along the midline using a robust loess algorithm—a weighted linear least squares second-order polynomial model that assigns lower weight to outliers (Savitzky and Golay, 1964), which performed best out of the algorithms we tested (see the Supplemental Material for details). Generating the trunk channel profile by smoothing rather than connecting the extrapolated confluence elevation points accommodates the uncertainty in the two-dimensional location of the paleo-valley.

We constructed the pre-flood valley topography by interpolating between the elevations of the reconstructed longitudinal profile of each paleo-trunk channel (i.e., trunk-channel long profile) and the rim on each side of the canyon



Downloaded from http://pubs.geoscienceworld.org/gsa/gsabulletin/article-pdf/136/9-10/4398/6900623/b36975.1.pdf?casa_token=IUGEppbvuJUAAAAA:cP-Iqvj09IGdMOx5aYgrxkIN0Y9yBKjypGEIlcxz3I4RsuNXqhxJW7HKJC
by Univ of Massachusetts Amherst user

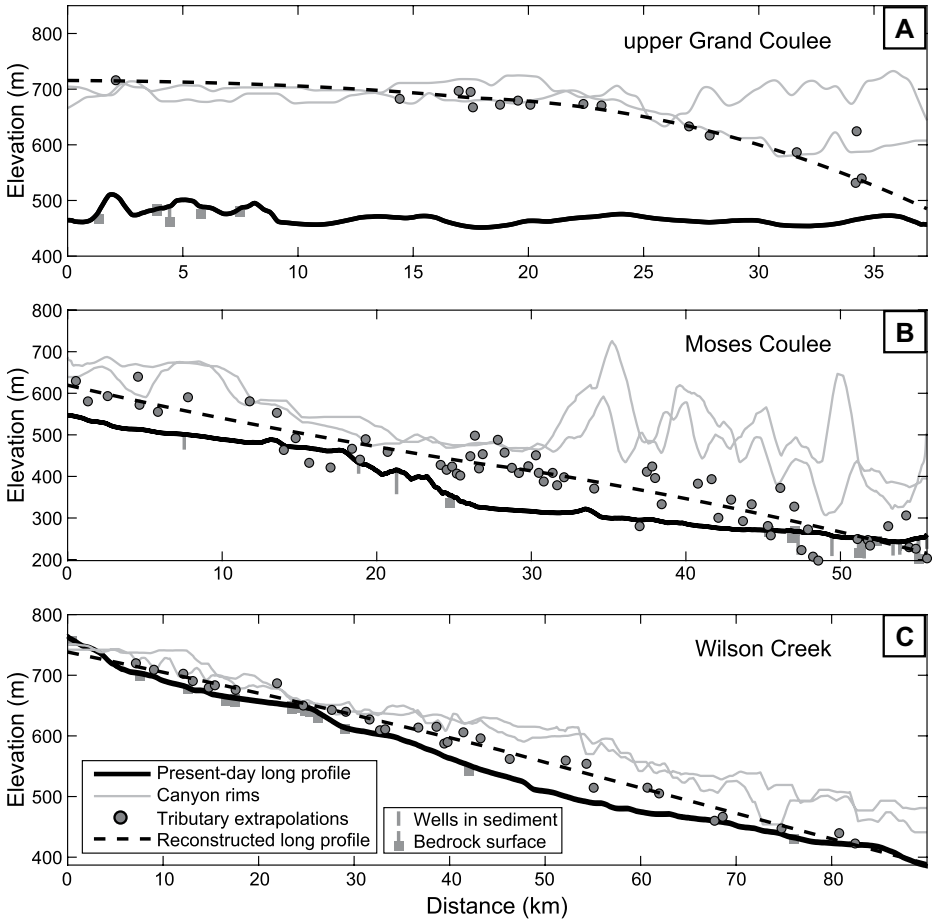


**Figure 3. Reconstructed long profiles for upper Grand Coulee (A), Moses Coulee (B), and Wilson Creek (C) in eastern Washington, USA, showing the present-day long profile (solid black line) and the top of the canyon or channel rims (gray lines), and the projected elevations of hanging tributaries (points), which were fit with a polynomial function that was smoothed to generate the reconstructed long profile (dashed line). Well log data indicating the minimum depth of sediment fill in each canyon is indicated by vertical gray lines, with squares indicating wells where the bedrock surface was encountered (see the Supplemental Material [text footnote 1] for details on well log data).**

or channel. The outline of each canyon or channel rim, which defined the limit of interpolation, was delineated manually using aerial imagery and DEM-derived slope maps. The canyon rims were discretized into points with 10 m spacing and were assigned their present-day elevation. A modified spline function that allows for abrupt changes in topography and enforces connected drainage paths (Wahba, 1990; Hutchinson et al., 2011) was used to interpolate elevations between the points along the rims and those along the reconstructed trunk-channel long profile. The interpolation process involved a maximum of 20 iterations and an elevation tolerance of 200 m to produce topography with a cell size of 10 m. A DEM with the reconstructed, pre-flood topography was generated by merging the interpolated topography over the present-day topography for each canyon or channel, keeping only the higher of the two elevations (Fig. S2). The volume of eroded rock, $V_r$ ($m^3$), was calculated as the sum of all elevation differences between the reconstructed pre-flood topography and the present-day topography, multiplied by the cell area. Our estimates of the volume of rock eroded from each flood channel do not account for post-flood erosion or deposition, and thus are minimum estimates. Post-flood erosion is thought to have caused only minor changes in canyon dimensions (Bretz, 1923). However, local deposition on the order of many tens of meters has been identified in Moses Coulee (Hanson, 1970). Deposition in Moses Coulee includes coarse-grained flood deposits, slackwater sediments deposited in the lower coulee due to backflooding from the Columbia River by floods in other channels, and post-flood glacial outwash. Additional details on sediment thickness and well log data are included in the Supplemental Material (Fig. S2).

We tested the topographic reconstruction methods by comparing reconstructed topography against the present-day topography in the Douglas Creek watershed, a tributary of Moses Coulee that was not eroded by floods. The error in the predicted thalweg elevation was a minor 2.8% of the total long profile relief, and modeled shear stresses on the reconstructed and real topography were similar, as expected. A complete description of the methods and results of error analysis and sensitivity testing in Douglas Creek are included in the Supplemental Material.

### Paleo-Discharge Reconstruction

Upper Grand Coulee eroded by retreat of an ~200 m tall vertical waterfall (Bretz, 1932) and Moses Coulee eroded by retreat of a broad knickpoint or cataract complex several km in length (Hanson, 1970; Larsen and Lamb, 2016). Whether Wilson Creek was eroded by a prominent knickpoint is unclear, but we assume that headward incision by plucking played a role in its incision for the purpose of calculating cataract retreat rates. Due to the field evidence for channel bed lowering during floods, we assume high-water evidence was emplaced while floods were flowing across the paleo-topography, before the canyons reached their present, post-flood depths (Larsen and Lamb, 2016; Lehnigk and Larsen, 2022).

To reconstruct the paleo-flood discharge in each canyon, we simulated outburst floods on both the reconstructed and present-day topography using ANUGA, a hydraulic modeling software that solves the two-dimensional shallow water equations (Roberts et al., 2015). ANUGA solves the flow equations on an irregular triangular mesh to optimize numerical efficiency and stability; the maximum cell size in our simulations was 5000 $m^2$. The purpose of these simulations was not to simulate the hydrograph of a flood from glacial Lake Missoula, but rather to conservatively determine the smallest discharge that just inundates specific high-water evidence. Therefore, a series of steady-state flood discharges were routed through each canyon to determine which discharge best matched high-water evidence for both the reconstructed and present-day topography using an approach similar to that of Lehnigk and Larsen (2022) and David et al. (2022). A range of discharges of interest for each canyon was simulated using a stair-step hydrograph, with periods of constant discharge separated by incremental stepwise increases in discharge. The discharge step incre-



Downloaded from http://pubs.geoscienceworld.org/gsa/gsabulletin/article-pdf/136/9-10/4398/6900623/b36975.1.pdf?casa_token=IUGEppbvuJUAAAAA:cP-Iqvj09IGdMOx5aYgrxkIN0Y9yBKjypGEIlcxz3I4RsuNXqhxJW7HKJC
by Univ of Massachusetts Amherst user

TABLE 1. SUMMARY OF MODEL RUNS TO CONSTRAIN HIGH-WATER-INUNDATING DISCHARGES IN THE CHANNELED SCABLAND, EASTERN WASHINGTON

| Lateral boundary conditions | High-water mark | Ranges of simulated discharges ($10^6$ $m^3s^{-1}$) | Discharge interval ($10^6$ $m^3s^{-1}$) | High-water-inundating discharge ($10^6$ $m^3s^{-1}$) |
|---|---|---|---|---|
| Upper Grand Coulee | | | | |
| Closed | Crossed drainage divide | Reconstructed:<br>0.25–0.5<br>0.55–1.25<br>1.5–3.0<br>3.05–3.25<br>3.5–5.0 | Reconstructed:<br>0.25<br>0.5<br>0.25<br>0.05<br>0.25 | Reconstructed:<br>3.1 |
| | | Present-day:<br>5–6<br>6.25*<br>6.5–6.75<br>7.0–8.0<br>10–20 | Present-day:<br>1<br><br>0.05<br>0.25<br>1 | Present-day:<br>14 |
| Moses Coulee | | | | |
| Closed | Scarp boulder and flood gravel | Reconstructed:<br>0.25*<br>0.5–1.25<br>1.5–2.5 | Reconstructed:<br><br>0.05<br>0.25 | Reconstructed:<br>0.65 (scarp boulder)<br>0.9 (flood gravel) |
| | | Present-day:<br>0.65*<br>0.9*<br>2.0–2.25<br>2.5–4.0<br>3.05–3.5 | Present-day:<br><br><br>0.05<br>0.25<br>0.05 | Present-day:<br>3.1 (scarp boulder)<br>2.2 (flood gravel) |
| Wilson Creek | | | | |
| Open | Streamlined basalt | Reconstructed:<br>0.05–1.0 | Reconstructed:<br>0.05 | Reconstructed:<br>0.9 |
| | | Present-day:<br>0.25–1 | Present-day:<br>0.05 | Present-day:<br>0.9 |
| Closed | Streamlined basalt | Reconstructed:<br>0.05–0.95 | Reconstructed:<br>0.05 | Reconstructed:<br>0.65 |
| | | Present-day:<br>0.25–1<br>1.1–1.2 | Present-day:<br>0.05<br>0.1 | Present-day:<br>0.8 |

*Indicates a single discharge rather than a range of discharges.

ments varied depending on the model domain, such that larger steps were used for larger discharges (Table 1). Periods of constant discharges were maintained for 150,000 s (41.67 h), which was sufficient or longer than required to achieve steady-state flow (Lehnigk and Larsen, 2022).

Water discharge was introduced from the upstream boundary of the modeling domain. Outlet boundary segments were modeled as Dirichlet boundaries with water levels >500 m lower than topography, so that flow encountering the boundary immediately exited the domain and the boundary did not produce a backwater effect (Larsen and Lamb, 2016). The inlet and certain lateral boundaries that were likely blocked by glacial ice (Bretz, 1932; Lehnigk and Larsen, 2022) were modeled as reflective boundaries (Fig. S3). The maximum distance over which drawdown effects from the Dirichlet outlet may have influenced modeled stages and shear stresses were estimated using methods outlined in Lamb et al. (2012) to be 15.2 km (upper Grand Coulee), 7.9 km (Moses Coulee, scarp boulder high-water mark), 8.3 km (Moses Coulee, flood gravel high-water mark), 7.8 km (Wilson Creek, lateral boundaries closed), and 8.3 km (Wilson Creek, lateral boundaries open), all of which are downstream of the high-water marks used. A spatially uniform Manning roughness coefficient of 0.065 s $m^{-1/3}$ was used, representative of roughness values previously estimated in Moses Coulee (Larsen and Lamb, 2016). Different roughness values cause only minor changes in reconstructed discharge, as discussed by Lehnigk and Larsen (2022).

For each simulation, we determined the smallest magnitude discharge at steady-state that inundated the geologic evidence of high water in each canyon. The high-water marks in all three canyons or channels provide minimum constraints on flood water-surface elevation and discharge, yet likely formed at shallow depths (Baker, 1978a; Bjornstad, 2014; O'Connor et al., 2020). In upper Grand Coulee, only one high-water mark was used: a shallow drainage divide crossed by floods near the eastern-most extent of local flooding that separates a loess hill from the adjacent loess-covered uplands (47.85010°N, 119.00920°W; elevation: 744 m; O'Connor et al., 2020; Fig. S4), which was also used by Lehnigk and Larsen (2022).

We evaluated high-water marks in two areas of Moses Coulee. In the lower portion, within a knickzone, we used the highest rounded, flood-transported boulder found at the base of an erosional scarp in loess (47.430867°N, 119.817633°W; elevation: 522 m; Larsen and Lamb, 2016; Fig. S5) and flood gravel on a mid-coulee butte (47.481909°N, 119.744475°W; elevation: 519 m; Washington State Department of Natural Resources, 2010; Fig. S6). We considered other high-water evidence in Moses Coulee, such as a flood bar deposited in a hanging tributary (Armor Draw; 47.584218°N, 119.698131°W; elevation: 618 m). However, our topographic reconstruction infilled the tributary mouth, which prevented us from determining the discharge that inundated the bar. We also evaluated the discharge required to inundate the Great Bar, the largest flood-depositional landform in Moses Coulee (47.591389°N, 119.688889°W; elevation: 582 m; Fig. S7), with a top that is 70 m above the coulee floor (which has been locally infilled by post-flood glacial outwash). The elevation of the base of the Great Bar is below that of the mouths of the hanging tributaries, indicating the bar was deposited after canyon incision. Hence, the discharge we reconstruct for the Great Bar provides a minimum estimate of the magnitude of floods that post-date canyon incision, which we compare against the magnitude of canyon-incising floods for Moses Coulee.

One high-water mark was used in Wilson Creek: a region of stripped basalt adjacent to loess streamlined by floodwaters that overtopped a drainage divide (47.63463°N, 118.91333°W; elevation: 613 m; O'Connor



Downloaded from http://pubs.geoscienceworld.org/gsa/gsabulletin/article-pdf/136/9-10/4398/6900623/b36975.1.pdf?casa_token=IUGEppbvuJUAAAAA:cP-Iqvj09IGdMOx5aYgrxkIN0Y9yBKjypGEIlcxz3I4RsuNXqhxJW7HKJC
by Univ of Massachusetts Amherst user

et al., 2020; Figs. S8 and S9). Flow through Wilson Creek can overtop drainage divides to the west and exit the model domain in the present-day topography. Hence, we ran two models for Wilson Creek—one with lateral boundaries open to flow and a second model with lateral boundaries closed—to account for the unknown state of erosion in neighboring drainage networks when flooding occurred. Results for models through upper Grand Coulee and Moses Coulee with open lateral boundaries are given in Table S5.

### Constraints on Erosion Rates and Number of Floods

In landscapes where outburst floods erode fractured bedrock, such as the Channeled Scabland, the rate at which blocks entrained by plucking are transported downstream can be the rate limiting step for canyon incision (Lamb and Fonstad, 2010; Lamb et al., 2015). Likewise, at waterfalls and cataracts where erosion is caused by toppling, erosion can be limited by sediment transport, otherwise talus will accumulate at the base of knickpoints and buttress them from headward erosion (Lamb et al., 2008; Lamb and Dietrich, 2009; Lapotre et al., 2016; Bender, 2022). Therefore, given estimates of the volume of rock eroded by floods, $V_r$, we predicted the number of floods required to incise bedrock canyons in well-fractured rock (Lamb et al., 2008; Lamb and Fonstad, 2010).

From mass balance, the number of floods necessary to incise each canyon ($N$) is (Lapotre et al., 2016):

$$N = \frac{T_f}{T_d} = \frac{V_r Q_s}{T_d}, \tag{2}$$

where $N$ is the number of floods responsible for the observed erosion, $T_f$ is the total duration of flooding required to remove all of the missing rock in the canyon, $T_d$ is the duration over which the flood is capable of erosion, and $Q_s$ is the volumetric sediment transport rate. The floods from glacial Lake Missoula were likely of different sizes and durations (Benito and O'Connor, 2003); however, our analysis considered only a single repeating representative (e.g., average) flood for purposes of reconstructing the floods from topographic change. The characteristic flood was assumed to have $T_d = 100$ h, the duration in which most of the flood energy is expended according to previous two-dimensional modeling that dynamically simulated drainage of glacial Lake Missoula through the Channeled Scabland at the maximum extent of the Okanogan ice lobe (Denlinger and O'Connell, 2010).

To estimate the sediment transport rate, $Q_s$, for the characteristic flood, we followed previous work and assumed that the sediment transport rate was set by sediment transport capacity, rather than the rate of bedrock erosion (Lamb et al., 2008; Lapotre et al., 2016). To calculate sediment transport capacity, we first needed to estimate the bed shear stress. To find the bed stress, we simulated a flood using ANUGA over the present-day topography with a discharge equal to that which just inundated high-water marks on the reconstructed topography, as this best approximates the topography in the wake of a retreating (but not fully eroded) knickpoint or cataract. We calculated the bed shear stresses, $\tau$ (Pa), for all cells as:

$$\tau = \rho g n^2 \overline{u}^2 h^{-\frac{1}{3}}, \tag{3}$$

where $\rho$ (1000 kg m$^{-3}$) is the density of water, $g$ (9.81 m s$^{-2}$) is acceleration due to gravity, $n$ (0.065 s m$^{-1/3}$) is the Manning roughness coefficient, $\overline{u}$ (m s$^{-1}$) is the modeled depth-averaged flow velocity, and $h$ (m) is the modeled flow depth. Depth-averaged velocity was calculated as $\overline{u} = \frac{(p_x^2 + p_y^2)^{\frac{1}{2}}}{h}$, where $p_x$ and $p_y$ are the $x$ and $y$ momentum, respectively, defined within ANUGA as the fluid momentum normalized by fluid density and cell width (Roberts et al., 2015). The sediment transport calculations used the median value of $\tau$ for cells with water depths greater than 0.5 m in a 10 km reach of each canyon starting 0.5–1 km upstream of the maximum distance estimated to be impacted by drawdown effects (Lamb et al., 2012; Figs. S10 and S11). Due to the >10 km maximum drawdown distance in upper Grand Coulee, the domain for the model using the high-water-inundating shear stress on the present-day topography in upper Grand Coulee was extended to ~30 km downstream from the Dry Falls cataract, so that any observed drawdown would be due to flow over the cataract rather than interaction with the model boundary. The standard error in shear stress was calculated as the standard deviation divided by the number of cells. The range of shear stresses spanned by the difference between the median and standard error defined the minimum and maximum values used to calculate transport rates.

We calculated the sediment transport capacity, $Q_{sed}$ (m$^3$ s$^{-1}$), as:

$$Q_{sed} = w(q_b + q_s), \tag{4}$$

where $q_b$ (m$^2$ s$^{-1}$) and $q_s$ (m$^2$ s$^{-1}$) are the volumetric bedload and suspended load transport capacities per unit width, and $w$ (m) is the mean canyon or channel width in the 10-km-long reach where shear stresses were extracted. To calculate bedload transport capacity, we used (Fernandez Luque and Van Beek, 1976):

$$q_b = 5.7\left(rgD^3\right)^{1/2}\left(\tau_* - \tau_{*c}\right)^{3/2}, \tag{5}$$

where $r = \frac{\rho_r - \rho}{\rho}$ ($\rho_r = 2800$ kg m$^{-3}$ is the density for basalt) is the relative density of basalt to water, $D$ is the grain diameter (m). The Shields stress is $\tau_* = \frac{\tau}{(\rho - \rho_r)gD}$, where $\tau$ (Pa) is the value of shear stress from Equation 3 averaged over the 10-km-long reach for each canyon. The critical value for transport was set to $\tau_{*c} = 0.045$ (Buffington and Montgomery, 1997).

Grain size was estimated from intermediate axis measurements of 220 clasts at 1 m spacing on the top of an abandoned channel bar on a terrace 70 m above the channel floor of Moses Coulee (Larsen and Lamb, 2016). The basalt clasts that comprise the bar are well-rounded, indicating bedload transport, and the majority of clasts are <0.5 m in diameter (Larsen and Lamb, 2016). Since armoring may lead to overestimation of grain sizes on bars in the Channeled Scabland (Atwater, 1987), we used the median measured grain diameter of 0.15 m as an upper bound, and a lower bound of 0.03 m that was calculated using an empirically determined armoring ratio of 4.8 (King, 2004, p. 200). We assumed the range of grain diameters is representative of all three canyons because the fracture spacing of the basalt bedrock is comparable throughout the study area (Reidel and Tolan, 2013).

Suspended sediment discharge per unit width ($q_s$) was calculated using the modeled bedload discharge and a suspended-to-bedload transport ratio. A suspended-to-bedload ratio of 8.3 was determined by dividing the volume of fine-grained offshore flood deposits by the volume of coarse-grained terrestrial flood deposits. We assume the 1450 km$^3$ of late Marine Isotope Stage 2 fine-grained deposits located offshore on the Astoria Fan (Normark and Reid, 2003) comprise the flood-generated suspended sediment. The offshore deposits do include contributions from loess stripped from the Columbia Plateau by floods, which is not attributable to bedrock erosion; however, this influence is compensated by the presence of terrestrial fine-grained flood deposits, which are not included in our analysis, and because the offshore sediment volume estimate is a minimum value (Normark and Reid, 2003). We assume mapped coarse-grained gravel comprise the flood-generated bedload sediment (Washington State Department of Natural Resources, 2010; Franczyk, et al., 2023). Applying a median thickness of 30 m to all



Downloaded from http://pubs.geoscienceworld.org/gsa/gsabulletin/article-pdf/136/9-10/4398/6900623/b36975.1.pdf?casa_token=IUGEppbvuJUAAAAA:cP-Iqvj09IGdMOx5aYgrxkIN0Y9yBKjypGEIlcxz3I4RsuNXqhxJW7HKJC
by Univ of Massachusetts Amherst user

mapped deposits, which is based on thickness values determined at 63 locations throughout the Channeled Scabland by Bretz (1919, 1928a, 1929, 1930) and Bretz et al. (1956), yields a total bedload volume of 175 km$^3$ (Table S6). Different ratios result in different predictions of flood numbers (Table S7).

To find the number of characteristic floods, we combined Equations 2–5. To find the average erosion rate per flood for each canyon or channel ($E$, m$^3$ s$^{-1}$), we used $E = \frac{V}{NT_d}$. Assuming all the erosion occurred by waterfall or cataract retreat, which is likely for Grand and Moses coulees (Bretz, 1923) but less clear for Wilson Creek, the retreat rate ($R$, m s$^{-1}$) for each canyon or channel was calculated as $R = \frac{L_c}{NT_d}$, where $L_c$ (m) is the canyon length. The shear stress values we used to model sediment transport for the characteristic flood are minimum estimates, because they are derived from the smallest discharge to inundate the high-water marks, which could bias our estimated number of floods to be too large and erosion rates too small. However, this uncertainty might be partially compensated for by the assumption that the floods were at transport capacity. If instead bedrock erosion was rate limiting, then this would bias our estimated number of floods too small and erosion rates too large.

We calculated a set of values for the number of floods, erosion rate, and knickpoint retreat rate for each combination of parameters, including the standard error in shear stress associated with each high-water mark and boundary condition (for Moses Coulee and Wilson Creek only), the median grain diameter assuming both bar armoring and no armoring, and the suspended-to-bedload transport ratio. Each combination of parameters generated an estimated number of floods, and we determined the median and 95th percentile of these estimates for each canyon to predict the range of the number of floods that contributed to the erosion of each canyon (Table S8). All calculated values for the number of floods were rounded up to the nearest whole number.

## RESULTS

### Topographic Reconstruction

Interpolation of pre-incision topography from the reconstructed long profiles (Fig. 3) produces the expected V-shaped fluvial valleys with thalweg profiles that slope in the downstream direction (Fig. 4), giving support for the reconstruction methodology. We found that the largest magnitude of erosion was in upper Grand Coulee where 67.8 km$^3$ of rock was eroded by floods, with most removal occurring in the upstream two-thirds of the canyon. In Moses Coulee, 14.5 km$^3$ of rock was eroded, primarily from the upstream section of the canyon. Wilson Creek experienced the smallest amount of incision, with 1.6 km$^3$ of rock eroded, largely along the channel center. The mean depth of erosion we calculated was 169 m for upper Grand Coulee, 56 m for Moses Coulee, and 10 m for Wilson Creek.

### Paleo-Discharge Reconstruction

Using the reconstructed pre-flood topography, the smallest flood discharge to inundate the high-water mark in upper Grand Coulee was $3.1 \times 10^6$ m$^3$ s$^{-1}$ (Fig. 4; Table 1). This calculation assumes that the high-water mark was emplaced prior to the majority of canyon incision. In contrast, matching the high-water mark over the present-day topography requires substantially more flow ($14 \times 10^6$ m$^3$ s$^{-1}$) in Grand Coulee. Likewise, in Moses Coulee, simulated discharges of 0.65 m$^3$ s$^{-1}$ and $0.9 \times 10^6$ m$^3$ s$^{-1}$ inundate the scarp boulder and flood gravel high-water marks, respectively, using the reconstructed pre-flood topography. Using the present-day topography required, again, much larger values of $3.1 \times 10^6$ m$^3$ s$^{-1}$ and $2.2 \times 10^6$ m$^3$ s$^{-1}$. Simulations indicate a discharge of $0.9 \times 10^6$ m$^3$ s$^{-1}$ inundates nearly all of the Great Bar in Moses Coulee, and the next-highest simulated discharge of $2.0 \times 10^6$ m$^3$ s$^{-1}$ fully inundates it. In Wilson Creek, the discharges that inundate high-water evidence on the reconstructed topography are $0.65 \times 10^6$ m$^3$ s$^{-1}$ and $0.9 \times 10^6$ m$^3$ s$^{-1}$ when the model boundaries are closed and open to flow, respectively. However, unlike the other sites, the values for Wilson Creek for the present-day topography ($0.8 \times 10^6$ m$^3$ s$^{-1}$ and $0.9 \times 10^6$ m$^3$ s$^{-1}$) were more similar to those on the reconstructed topography.

### Sediment Transport and Erosion Rates

The median bed shear stresses in the 10 km reaches using the present-day topography were $2276 \pm 5$ Pa for a discharge of $3.1 \times 10^6$ m$^3$ s$^{-1}$ in upper Grand Coulee, $1049 \pm 5$ Pa and $1180 \pm 6$ Pa for Moses Coulee (for the smallest discharge to inundate the scarp boulder and flood gravel, $0.65 \times 10^6$ m$^3$ s$^{-1}$ and $0.9 \times 10^6$ m$^3$ s$^{-1}$, respectively), and $157 \pm 7$ Pa and $174 \pm 6$ Pa for Wilson Creek (for the smallest discharge to inundate the stripped basalt with lateral boundaries open and closed, $0.65 \times 10^6$ m$^3$ s$^{-1}$ and $0.9 \times 10^6$ m$^3$ s$^{-1}$, respectively; Fig. S10). Despite having the same high-water-inundating discharges, the shear stresses generated in the 10-km-long reach of Moses Coulee were several times higher than those generated for the equivalent section of Wilson Creek, likely because the inundation in Moses Coulee is narrower than Wilson Creek (average width of 2.1 versus 5.1 km) in the corresponding portion of the channel.

Using the discharge or set of discharges predicted for each canyon or flood channel to match high-water marks on the reconstructed pre-flood topography, and assuming that flows exceeded erosion and transport thresholds for 100 h per flood, we predicted that it took $6 \pm 1$, $6 \pm 2$, and $13 \pm 14$ floods ($\pm$ values indicate 95th percentile uncertainty) to erode upper Grand Coulee, Moses Coulee, and Wilson Creek, respectively. Volumetric erosion rates calculated as ranges defined by the 5th and 95th percentile estimates are 32,830–35,200 m$^3$ s$^{-1}$ for upper Grand Coulee, 5580–8260 m$^3$ s$^{-1}$ for Moses Coulee, and 170–4350 m$^3$ s$^{-1}$ for Wilson Creek. Assuming all erosion occurred via waterfall retreat, the waterfall retreat rates per flood were 2280–2440 m day$^{-1}$ for upper Grand Coulee, 2320–3430 m day$^{-1}$ for Moses Coulee, and 680–17,930 m day$^{-1}$ for Wilson Creek (Fig. 5).

## DISCUSSION

### Topographic and Discharge Reconstruction

Bretz (1932, p. 82) estimated that "about eight cubic miles of rock," or ~33 km$^3$, had been eroded from upper Grand Coulee by floods. Our estimate of flood-induced bedrock erosion is approximately twice that value. Although Hanson (1970, p. 124) generated contours of bedrock erosion in Moses Coulee, the total volume of eroded rock was not calculated. However, the pattern of erosion predicted by our method is similar to that predicted by Hanson (1970), with the greatest erosion occurring in the narrow upper and lower canyon reaches of Moses Coulee and minimal erosion in middle reach, where the width is greatest (Fig. 4). There are no prior estimates of erosion for Wilson Creek. Hence, our results place new estimates on the volume of rock eroded from these channels by the floods from glacial Lake Missoula. The median shear stresses in Wilson Creek are an order of magnitude lower than those predicted in upper Grand Coulee and Moses Coulee, despite having a similar predicted discharge range to Moses Coulee on reconstructed topography. The lack of major geological structures, and hence topographic relief and associated rock fracturing, prevented development of a major retreating waterfall or cataract in Wilson Creek. Hence, although we calculate cataract retreat rates from



Downloaded from http://pubs.geoscienceworld.org/gsa/gsabulletin/article-pdf/136/9-10/4398/6900623/b36975.1.pdf?casa_token=IUGEppbvuJUAAAAA:cP-Iqvj09IGdMOx5aYgrxkIN0Y9yBKjypGEIlcxz3I4RsuNXqhxJW7HKJC
by Univ of Massachusetts Amherst user

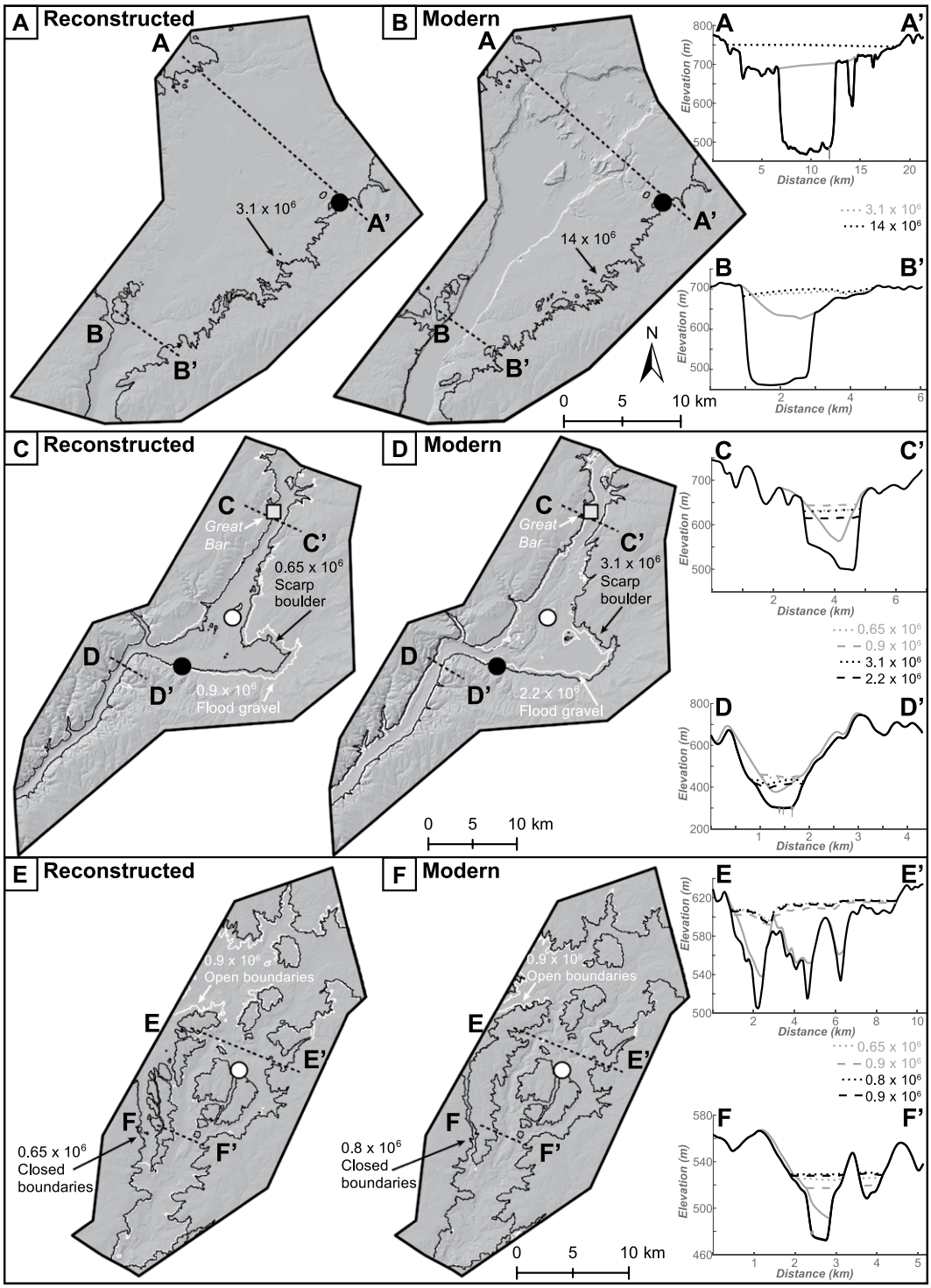


**Figure 4. Hillshade images of reconstructed pre-flood topography (A, C, and E) and flood-eroded present-day topography (B, D, and F) for upper Grand Coulee (A and B), Moses Coulee (C and D), and Wilson Creek (E and F) in eastern Washington, USA, with the extent of inundation for the lowest discharge that inundated a given high-water mark delineated as a black line. Two cross sections are included for each canyon; the present-day topography is shown with a solid black line, and the reconstructed topography is shown with a solid gray line. Water surface profiles for the lowest discharge that inundated a given high-water mark are delineated as dashed or dotted lines on the cross sections. Discharges are in units of $m^3$ $s^{-1}$. Minimum sediment depths from well logs near cross sections are indicated by vertical gray lines, with squares indicating wells where the bedrock surface was encountered (see the Supplemental Material [text footnote 1] for details on well log data).**

Wilson Creek, the values are likely not physically realistic.

The paleo-discharge values we reconstruct for Moses Coulee based on topographic reconstruction and high-water evidence are nearly identical to independent estimates based on the assumption that canyons incise into fractured bedrock when bed shear stresses just exceed the threshold for erosion by block plucking (Larsen and Lamb, 2016). Larsen and Lamb (2016) reconstructed the topography in Moses Coulee by extrapolating the elevations of erosional surfaces defined by basalt flow bedding horizontally across the canyon, and found that a discharge of $0.6 \times 10^6$ $m^3$ $s^{-1}$ generated sufficient shear stresses to erode the canyon. A discharge of $0.6 \times 10^6$ $m^3$ $s^{-1}$ is essentially the same as the value of $0.65 \times 10^6$ $m^3$ $s^{-1}$ that we infer for the same location, especially given that Larsen and Lamb (2016) only simulated discharge in larger ($0.1 \times 10^6$ $m^3$ $s^{-1}$) increments. A discharge of $0.6–0.65 \times 10^6$ $m^3$ $s^{-1}$ is substantially lower than discharge estimates that infer the present-day topography was filled to the canyon brim with water, which we



Downloaded from http://pubs.geoscienceworld.org/gsa/gsabulletin/article-pdf/136/9-10/4398/6900623/b36975.1.pdf?casa_token=IUGEppbvuJUAAAAA:cP-Iqvj09IGdMOx5aYgrxkIN0Y9yBKjypGEIlcxz3I4RsuNXqhxJW7HKJC
by Univ of Massachusetts Amherst user

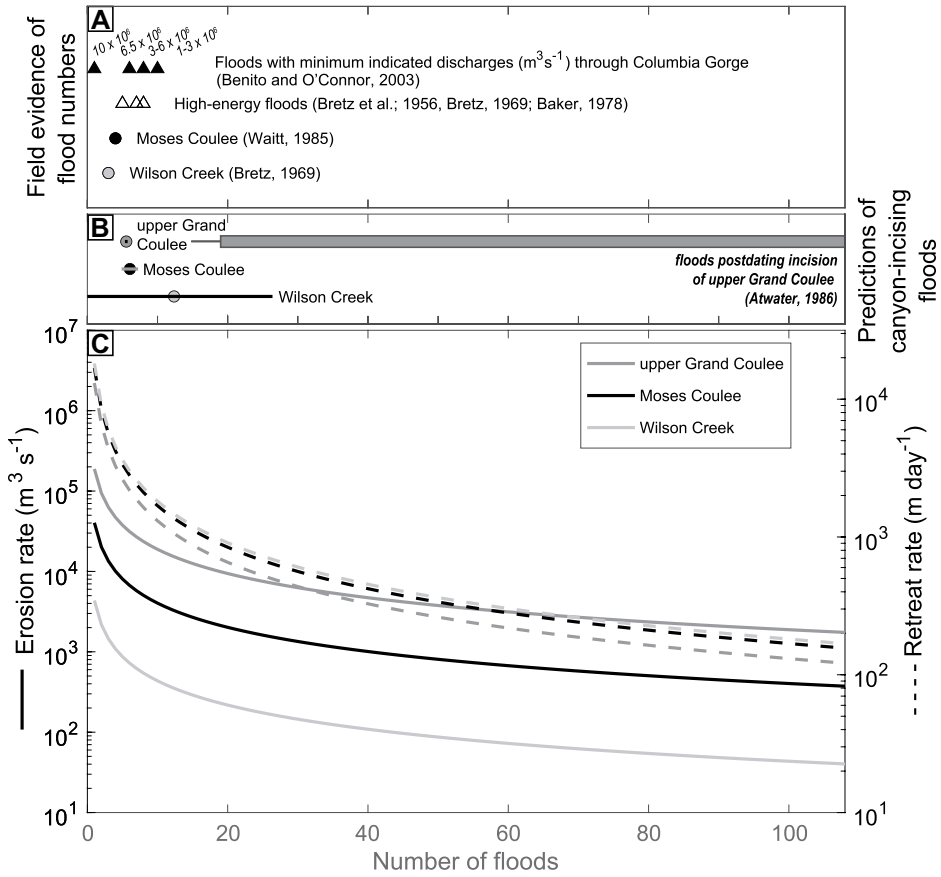


**Figure 5. (A) Field-based estimates of flood numbers for locations throughout the Channeled Scabland, eastern Washington, USA. (B) Predicted numbers of floods (horizontal bars span 95th percentile and are smaller than some of the symbols). The gray bar extending from the right-hand side of the plot indicates the 89 floods through upper Grand Coulee that post-date canyon incision (Atwater, 1986), using either 108 floods (thick bar) or 104 floods (thin line) as the total number of floods (O'Connor et al., 2020). (C) Predicted erosion rates (solid lines), waterfall or cataract retreat rates (dashed lines).**

infer was up to $3.1 \times 10^6$ m$^3$ s$^{-1}$, but has been previously been estimated to be on the order of $10 \times 10^6$ m$^3$ s$^{-1}$ (Hanson, 1970; Harpel, 1996; Harpel et al., 2000). The flood discharge inferred to inundate the Great Bar in Moses Coulee is slightly greater than $0.9 \times 10^6$ m$^3$ s$^{-1}$, which is similar to the discharge required to inundate the flood-gravel high-water evidence in Moses Coulee. Hence, in Moses Coulee, the discharges that drove canyon incision may have been of similar magnitude to subsequent flows through the entrenched coulee.

The $3.1 \times 10^6$ m$^3$ s$^{-1}$ discharge we reconstruct for upper Grand Coulee is comparable to the value recently estimated using a different method of topographic reconstruction. Lehnigk and Larsen (2022) reconstructed the pre-flood topography in upper Grand Coulee by interpolating topography between the canyon rims upstream of a partially retreated waterfall, and found that a discharge of $2.6 \times 10^6$ m$^3$ s$^{-1}$ was sufficient to inundate high-water mark evidence and drive canyon incision by generating shear stresses large enough to topple rock columns at the waterfall face. The consistency of these results strongly indicates that upper Grand Coulee was eroded by a flood with discharge on the order of $3 \times 10^6$ m$^3$ s$^{-1}$. A discharge of $3 \times 10^6$ m$^3$ s$^{-1}$ is much lower than the discharge of $14 \times 10^6$ m$^3$ s$^{-1}$ we infer for brimful flow in the present-day upper Grand Coulee topography, which is comparable to prior estimates of 12–14 $10^6$ m$^3$ s$^{-1}$ determined using one-dimensional step-backwater modeling (Harpel, 1996; Harpel et al., 2000; Waitt et al., 2000).

Our discharge estimates, which are based on a more robust method of reconstructing pre-flood topography than prior work in the Channeled Scabland (Hanson, 1970; Larsen and Lamb, 2016), support the conclusion that modest-sized outburst floods of only a few million m$^3$ s$^{-1}$ were capable of carving the largest canyons into the Columbia Plateau (Larsen and Lamb, 2016; Lehnigk and Larsen, 2022). The canyon-carving discharges we infer are still exceptionally large relative to the present-day flow of the Columbia River, but the flood discharges we infer for the reconstructed topography are only a fraction—22% and 21%–40% for upper Grand Coulee and Moses Coulee, respectively—of the discharge that is required to fill the present-day canyon topography to the high-water marks. Hence, canyon-filling floods are not required to generate large-scale erosion and deep incision. The similarity in the results from this study and from Lehnigk and Larsen (2022), which are based on topographic reconstruction and high-water evidence, to those of Larsen and Lamb (2016), which are based on plucking thresholds alone, indicates that assessing plucking thresholds and the discharges that exceed them provides a robust and alternative method to reconstructing discharge using high-water evidence, especially in landscapes where pre-flood topography and high-water evidence is difficult to reconstruct.

### Rates of Waterfall Retreat and Erosion

The erosion rates inferred by our analyses indicate the landscape of the Columbia Plateau responded rapidly to flooding. If all the erosion in Grand and Moses coulees occurred by headward waterfall or cataract retreat, we predict retreat rates on the order of a kilometer or more per day. Knickpoint retreat rates inferred for other outburst flood-carved canyons carved into basalt have been estimated to be hundreds of meters over the course of several days (O'Connor, 1993; Lamb et al., 2008; Baynes et al., 2015b). Hence, the retreat rates are reasonable compared to those from other outburst floods that have occurred in landscapes with fractured bedrock, but cataracts in the Channeled Scabland may have retreated much more rapidly than other documented cases. At the source, just downstream from the ice dam, the floods from glacial Lake Missoula generated some the largest discharges of water in Earth's history (O'Connor et al., 2022) that have been estimated to be $17 \times 10^6$ m$^3$ s$^{-1}$ (O'Connor and Baker, 1992). As the floodwaters overtopped the Columbia River valley and were distributed across the Columbia Plateau, this study and our prior work (Larsen and Lamb, 2016; Lehnigk and Larsen, 2022) indicate individual flood routes conveyed much lower discharges of a few million m$^3$ s$^{-1}$ or less. Despite these lower discharges, our analysis of cataract retreat suggests the erosion of the fractured and jointed basalt occurred at rates that were potentially also among the most rapid that have occurred on Earth.



Downloaded from http://pubs.geoscienceworld.org/gsa/gsabulletin/article-pdf/136/9-10/4398/6900623/b36975.1.pdf?casa_token=IUGEppbvuJUAAAAA:cP-Iqvj09IGdMOx5aYgrxkIN0Y9yBKjypGEIlcxz3I4RsuNXqhxJW7HKJC
by Univ of Massachusetts Amherst user

### The Number of Canyon-Carving Floods

Determining the number of floods that formed the Channeled Scabland has long been a topic of inquiry. It was initially thought that a single flood formed the Channeled Scabland (Bretz, 1923). The number of floods was then revised to seven or eight (Bretz et al., 1956; Bretz, 1969), and later to five (Baker, 1978b). Investigation of slackwater deposits in subsequent decades indicated that glacial Lake Missoula experienced at least dozens of outburst floods, on the basis of graded bedding and other sedimentary evidence (e.g., Waitt, 1980, 1985; Atwater, 1986). The origin of the slackwater deposits and the interpretation that each graded bed was deposited by a single flood was later debated (Baker and Bunker, 1985; Waitt, 1985), but the current consensus is that beds in different stratigraphic sections represent ~100 individual floods (O'Connor et al., 2020). However, the proportion of those ~100 floods that had sufficiently high discharge to contribute to bedrock erosion and canyon incision is unclear (e.g., Baker and Bunker, 1985) and the preservation of slackwater deposits in areas predicted to have high bed shear stress during large floods (Smith, 2006; Alho et al., 2010) and upward fining and thinning of rhythmites suggest some slackwater deposits are from smaller floods that postdate canyon incision (Waitt and Atwater, 1989). Atwater (1986) documented 89 floods from glacial Lake Missoula through upper Grand Coulee from slackwater deposits upstream that post-date incision of the canyon; with a total of 104–108 floods from glacial Lake Missoula (O'Connor et al., 2020), this would leave a maximum of 15–19 floods to predate upper Grand Coulee's incision. Our estimate of $6 \pm 1$ canyon-incising floods in upper Grand Coulee is consistent with the constraint that 15–19 or fewer floods pre-date canyon incision (Fig. 5). Additionally, since flood pathways changed in response to changing topography and ice margins (Balbas et al., 2017; O'Connor et al., 2020; Denlinger et al., 2021; Pico et al., 2022), slackwater deposits found in downstream reaches and marine deposits cannot be attributed to flooding through individual canyons (Waitt, 1980, 1985; Clague et al., 2003; Gombiner et al., 2016). Even evidence of high energy floods from the Columbia Gorge, where sedimentary deposits and hydraulic modeling indicate there were at least 25 floods with peak discharges $>1–3 \times 10^6$ $m^3\ s^{-1}$ (Benito and O'Connor, 2003), cannot resolve the number of floods that contributed to the erosion of any particular canyon.

Our results place constraints on the number of characteristic floods that could have carved flood channels on the Columbia Plateau, and suggest that <10% of the ~100 documented floods played a role in eroding the largest canyons in the Channeled Scabland. At Moses Coulee, the only major canyon where there is clear evidence of the number of floods (Waitt, 1985), our prediction of $6 \pm 2$ floods is consistent with the field-based estimate of at least four large floods (Waitt, 2016; O'Connor et al., 2020). Hence, despite the assumptions we have made in our analysis and expected variability in parameters such as flood discharge, duration, and bedload dimensions, the similarity between our predictions and field-based estimates of flood numbers for Moses Coulee suggests our method provides a reasonable first-order estimate of the number of floods that contributed substantially to landscape evolution in the Channeled Scabland by carving deep canyons.

## CONCLUSIONS

Using hanging tributaries to reconstruct pre-flood topography, we estimate that floods from glacial Lake Missoula eroded a combined 83.9 $km^3$ of rock from upper Grand Coulee, Moses Coulee, and Wilson Creek, with the highest magnitude of erosion occurring where retreating waterfalls or cataracts developed. Flood discharges estimated through the pre-incision topography in the largest canyons are ~20%–40% of the discharges required to inundate the same high-water marks on the present-day topography, and are consistent with previous discharge estimates for upper Grand Coulee and Moses Coulee that used simpler methods to reconstruct the topography initially encountered by floods. Predictions based on shear stresses generated by the simulated floods and sediment transport modeling indicate that the two largest canyons in the Channeled Scabland could have been eroded by only half a dozen floods. Hence, our analysis suggests that the largest canyons in the Channeled Scabland were eroded by outburst floods with discharges on the order of a few million $m^3\ s^{-1}$ or less, but with exceptionally high erosion rates that formed the canyons over cumulative time scales of only a few weeks.

#### ACKNOWLEDGMENTS

The authors would like to thank E. Thaler for helpful conversations and coding assistance, N. Tull for assistance with ANUGA, A. Wickert and E. Baynes for formal reviews, J. O'Connor for helpful comments, and attendees of the Geological Society of America Penrose Conference for thought-provoking discussion. The authors also acknowledge the historical and present significance of the regions of the Channeled Scabland referenced in this study to the Confederated Tribes of the Colville Reservation—composed of members of the Chelan, Nez Perce, Colville, Entiat, Lakes, Methow, Moses-Columbia, Nespelem, Okanogan, Palus, San Poil, and Wenatchi tribes. This work was supported by a National Science Foundation (NSF) Graduate Research Fellowship to K.E. Lehnigk and a collaborative NSF Grant (1529528, 1529110) to I.J. Larsen and M.P. Lamb. Digital elevation data are available from the University of Washington Geomorphological Research Group website (http://gis.ess.washington.edu/data/). Please visit https://doi.org/10.7275/8zws-f751 to access archived data files and code.

#### REFERENCES CITED

Alho, P., Baker, V.R., and Smith, L.N., 2010, Paleohydraulic reconstruction of the largest Glacial Lake Missoula draining(s): Quaternary Science Reviews, v. 29, p. 3067–3078, https://doi.org/10.1016/j.quascirev.2010.07.015.

Anton, L., Mather, A.E., Stokes, M., Muñoz-Martin, A., and Vicente, G.D., 2015, Exceptional river gorge formation from unexceptional floods: Nature Communications, v. 6, no. 7963, https://doi.org/10.1038/ncomms8963.

Atwater, B.F., 1984, Periodic floods from glacial Lake Missoula into the Sanpoil arm of glacial Lake Columbia, northeastern Washington: Geology, v. 12, p. 464–467, https://doi.org/10.1130/0091-7613(1984)12<464:PFFGLM>2.0.CO;2.

Atwater, B.F., 1986, Pleistocene glacial-lake deposits of the Sanpoil River Valley, northeastern Washington: U.S. Geological Survey Bulletin, v. 1661, 48 p.

Atwater, B.F., 1987, Status of glacial Lake Columbia during the last floods from glacial Lake Missoula: Quaternary Research, v. 27, p. 182–201, https://doi.org/10.1016/0033-5894(87)90076-7.

Baker, V.R., 1973, Paleohydrology and Sedimentology of Lake Missoula Flooding in Eastern Washington: Geological Society of America Special Paper 144, 79 p., https://doi.org/10.1130/SPE144-p1.

Baker, V.R., 1978a, Paleohydraulics and hydrodynamics of Scabland floods, *in* Baker, V.R., and Nummedal, D., eds., The Channeled Scabland: A Guide to the Geomorphology of the Columbia Basin, Washington, Prepared for the Comparative Planetary Geology Field Conference Held in the Columbia Basin, June 5–8, 1978: National Aeronautics and Space Administration, p. 59–79, https://ntrs.nasa.gov/search.jsp?R=19780019525.

Baker, V.B., 1978b, Quaternary geology of the Channeled Scabland and adjacent areas, *in* The Channeled Scabland: A Guide to the Geomorphology of the Columbia Basin, Washington: U.S. National Aeronautics and Space Administration, Comparative Planetary Geology Field Conference, Columbia Basin, Washington, USA, 5–8 June, p. 17–35.

Baker, V.R., 1978c, The Spokane flood controversy and the Martian outflow channels: Science, v. 202, p. 1249–1256, https://doi.org/10.1126/science.202.4374.1249.

Baker, V.R., 1982, The Channels of Mars: Austin, Texas, University of Texas Press, 198 p.

Baker, V.R., and Bunker, R.C., 1985, Cataclysmic Late Pleistocene flooding from glacial Lake Missoula: A review: Quaternary Science Reviews, v. 4, p. 1–41, https://doi.org/10.1016/0277-3791(85)90027-7.

Baker, V.R., and Kale, V.S., 1998, The role of extreme floods in shaping bedrock channels, *in* Tinkler, K.J., and Wohl, E.E., eds., Rivers over Rock: Fluvial Processes in Bedrock Channels: AGU Geophysical Monograph 107, p. 153–165, https://doi.org/10.1029/GM107p0153.

Baker, V.R., Strom, R.G., Gulick, V.C., Kargel, J.S., Komatsu, G., and Kale, V.S., 1991, Ancient oceans, ice sheets and the hydrological cycle on Mars: Nature, v. 352, p. 589–594, https://doi.org/10.1038/352589a0.

Balbas, A.M., Barth, A.M., Clark, P.U., Clark, J., Caffee, M., O'Connor, J., Baker, V.R., Konrad, K., and Bjornstad, B., 2017, $^{10}$Be dating of late Pleistocene megafloods and Cordilleran Ice Sheet retreat in the northwestern United States: Geology, v. 45, p. 583–586, https://doi.org/10.1130/G38956.1.

Barry, T.L., Kelley, S.P., Reidel, S.P., Camp, V.E., Self, S., Jarobe, N.A., Duncan, R.A., and Renne, P.R., 2013, Eruption chronology of the Columbia River Basalt Group, *in* Reidel, S.P., Camp, V.E., Ross, M.E., Wolff, J.A., Martin, B.S., Tolan, T.L., and Wells, R.E., eds., The Columbia River Flood Basalt Province: Geologi-



Downloaded from http://pubs.geoscienceworld.org/gsa/gsabulletin/article-pdf/136/9-10/4398/6900623/b36975.1.pdf?casa_token=IUGEppbvuJUAAAAA:cP-Iqvj09IGdMOx5aYgrxkIN0Y9yBKjypGEIlcxz3I4RsuNXqhxJW7HKJC
by Univ of Massachusetts Amherst user

cal Society of America Special Paper 497, p. 45–66, https://doi.org/10.1130/2013.2497(02).

Baynes, E., Attal, M., Dugmore, A.J., Kirstein, L.A., and Whaler, K.A., 2015a, Catastrophic impact of extreme flood events on the morphology and evolution of the lower Jökulsá á Fjöllum (northeast Iceland) during the Holocene: Geomorphology, v. 250, p. 422–436, https://doi.org/10.1016/j.geomorph.2015.05.009.

Baynes, E., Attal, M., Niedermann, S., Kirstein, L.A., Dugmore, A.J., and Naylor, M., 2015b, Erosion during extreme flood events dominates Holocene canyon evolution in northeast Iceland: Proceedings of the National Academy of Sciences of the United States of America, v. 112, p. 2355–2360, https://doi.org/10.1073/pnas.1415443112.

Bender, A.M., 2022, Bedrock gorge incision via anthropogenic meander cutoff: Geology, v. 50, p. 321–325, https://doi.org/10.1130/G49479.1.

Benito, G., and O'Connor, J.E., 2003, Number and size of last-glacial Missoula floods in the Columbia River valley between the Pasco Basin, Washington, and Portland, Oregon: Geological Society of America Bulletin, v. 115, p. 624–638, https://doi.org/10.1130/0016-7606(2003)115<0624:NASOLM>2.0.CO;2.

Bishop, P., and Goldrick, P., 2000, Geomorphological evolution of the East Australian continental margin, *in* Summerfield, M.A., ed., Geomorphology and Global Tectonics: Chichester, UK, Wiley, p. 227–255.

Bjornstad, N., 2014, Ice-rafted erratics and bergmounds from Pleistocene outburst floods, Rattlesnake Mountain, Washington, USA: E&G Quaternary Science Journal, v. 63, p. 44–59, https://doi.org/10.3285/eg.63.1.03.

Bretz, J.H., 1919, The late Pleistocene submergence in the Columbia Valley of Oregon and Washington: The Journal of Geology, v. 27, p. 489–506, https://doi.org/10.1086/622675.

Bretz, J.H., 1923, The Channeled Scablands of the Columbia Plateau: The Journal of Geology, v. 31, p. 617–649, https://doi.org/10.1086/623053.

Bretz, J.H., 1928a, Bars of Channeled Scabland: Geological Society of America Bulletin, v. 39, p. 643–701, https://doi.org/10.1130/GSAB-39-643.

Bretz, J.H., 1928b, The Channeled Scabland of Eastern Washington: Geographical Review, v. 18, p. 446–477, https://doi.org/10.2307/208027.

Bretz, J.H., 1929, Valley deposits immediately east of the Channeled Scabland of Washington: The Journal of Geology, v. 37, p. 393–427, https://doi.org/10.1086/623636.

Bretz, J.H., 1930, Valley deposits immediately west of the Channeled Scabland: The Journal of Geology, v. 38, p. 385–422, https://doi.org/10.1086/623737.

Bretz, J.H., 1932, The Grand Coulee: New York, American Geographical Society, v. 15, 89 p.

Bretz, J.H., 1969, The Lake Missoula Floods and the Channeled Scabland: The Journal of Geology, v. 77, p. 505–543, https://doi.org/10.1086/627452.

Bretz, J.H., Smith, H.T.U., and Neff, G.E., 1956, Channeled Scabland of Washington: New data and interpretations: Geological Society of America Bulletin, v. 67, p. 957–1049, https://doi.org/10.1130/0016-7606(1956)67[957:CSOWND]2.0.CO;2.

Brocklehurst, S.H., and Whipple, K.X., 2006, Assessing the relative efficiency of fluvial and glacial erosion through simulation of fluvial landscapes: Geomorphology, v. 75, p. 283–299, https://doi.org/10.1016/j.geomorph.2005.07.028.

Buffington, J.M., and Montgomery, D.R., 1997, A systematic analysis of eight decades of incipient motion studies, with special reference to gravel-bedded rivers: Water Resources Research, v. 33, p. 1993–2029, https://doi.org/10.1029/96WR03190.

Clague, J.J., Barendregt, R., Enkin, R.J., and Foit, F.F., 2003, Paleomagnetic and tephra evidence for tens of Missoula floods in southern Washington: Geology, v. 31, p. 247–250, https://doi.org/10.1130/0091-7613(2003)031<0247:PATEFT>2.0.CO;2.

Clarke, G.K.C., Leverington, D.W., Teller, J.T., and Dyke, A.S., 2004, Paleohydraulics of the last outburst flood from glacial Lake Agassiz and the 8200 BP cold event: Quaternary Science Reviews, v. 23, p. 389–407, https://doi.org/10.1016/j.quascirev.2003.06.004.

Clubb, F.J., Weir, E.F., and Mudd, S.M., 2022, Continuous measurements of valley floor width in mountainous landscapes: Earth Surface Dynamics, v. 10, p. 437–456, https://doi.org/10.5194/esurf-10-437-2022.

Cook, K.L., Andermann, C., Gimbert, F., Adhikari, B.R., and Hovius, N., 2018, Glacial lake outburst floods as drivers of fluvial erosion in the Himalaya: Science, v. 362, p. 53–57, https://doi.org/10.1126/science.aat4981.

David, S.R., Larsen, I.J., and Lamb, M.P., 2022, Narrower paleo-canyons downsize megafloods: Geophysical Research Letters, v. 49, no. 11, https://doi.org/10.1029/2022GL097861.

Denlinger, R.P., and O'Connell, D.R.H., 2010, Simulations of cataclysmic outburst floods from Pleistocene Glacial Lake Missoula: Geological Society of America Bulletin, v. 122, p. 678–689, https://doi.org/10.1130/B26454.1.

Denlinger, R.P., George, D.L., Cannon, C.M., O'Connor, J.E., and Waitt, R.B., 2021, Diverse cataclysmic floods from Pleistocene glacial Lake Missoula, *in* Waitt, R.B., Thackray, G.D., and Gillespie, A.R., eds., Untangling the Quaternary Period—A Legacy of Stephen C. Porter: The Geological Society of America Special Paper 548, p. 333–350, https://doi.org/10.1130/2021.2548(17).

Ehlers, J., Gibbard, P.L., and Hughes, P.D., 2011, Quaternary Glaciations—Extent and Chronology: Amsterdam, Elsevier, v. 15, 1126 p.

Fernandez Luque, R., and Van Beek, R., 1976, Erosion and transport of bed-load sediment: Journal of Hydraulic Research, v. 14, p. 127–144, https://doi.org/10.1080/00221687609499677.

Flint, J.J., 1974, Stream gradient as a function of order, magnitude, and discharge: Water Resources Research, v. 10, p. 969–973, https://doi.org/10.1029/WR010i005p00969.

Fox, M., 2019, A linear inverse method to reconstruct paleo-topography: Geomorphology, v. 337, p. 151–164, https://doi.org/10.1016/j.geomorph.2019.03.034.

Franczyk, J.J., Madin, I.P., Duda, C.J.M., and McClaughry, J.D., 2023, Oregon Geologic Data Compilation release 7 (OGDC-7): Oregon Department of Geology and Mineral Industries, Digital Data Series GIS data, https://pubs.oregon.gov/dogami/dds/p-OGDC-7.htm.

Goldrick, G., and Bishop, P., 2007, Regional analysis of bedrock stream long profiles: Evaluation of Hack's SL form, and formulation and assessment of an alternative (the DS form): Earth Surface Processes and Landforms, v. 32, p. 649–671, https://doi.org/10.1002/esp.1413.

Gombiner, J.H., Hemming, S.R., Hendy, I.L., Bryce, J.G., and Blichert-Toft, J., 2016, Isotopic and elemental evidence for scabland flood sediments offshore Vancouver Island: Quaternary Science Reviews, v. 139, p. 129–137, https://doi.org/10.1016/j.quascirev.2016.02.026.

Hack, J.T., 1957, Studies of longitudinal stream profiles in Virginia and Maryland: U.S. Geological Survey Professional Paper 294-B, p. 45–97, https://doi.org/10.3133/pp294B.

Hack, J.T., 1973, Stream-profile analysis and stream-gradient index: Journal of Research of the U.S. Geological Survey, v. 1, p. 421–429.

Hanson, L.G., 1970, The origin and development of Moses Coulee and other scabland features on the Waterville Plateau, Washington [Ph.D. thesis]: Seattle, Washington, University of Washington, 140 p.

Harpel, C.J., 1996, Paleodischarges and inferred hydraulics of the Missoula Floods: Columbia River Valley and Channeled Scabland, Eastern Washington [Undergraduate thesis]: Bellingham, Washington, Western Washington University, 33 p.

Harpel, C.J., Waitt, R.B., and O'Connor, J.E., 2000, Paleodischarges of the late Pleistocene Missoula floods, eastern Washington, USA: Orkustofnun Rept. OS-2000/036, Reykjavík, Iceland, Extremes of the Extremes Conference, p. 21.

Howard, A.D., and Kerby, G., 1983, Channel changes in badlands: Geological Society of America Bulletin, v. 94, p. 739–752, https://doi.org/10.1130/0016-7606(1983)94<739:CCIB>2.0.CO;2.

Hutchinson, M.F., Xu, T., and Stein, J.A., 2011, Recent progress in the ANUDEM elevation gridding procedure, *in* Hengl, T., Evans, I.S., Wilson, J.P., and Gould, M., eds., Geomorphometry 2011 Conference, Redlands, California, p. 19–22.

King, J.G., 2004, Sediment transport data and related information for selected coarse-bed streams and rivers in Idaho: Department of Agriculture, Forest Service General Technical Report RMRS-GTR-131, 26 p.

Lamb, M.P., and Dietrich, W.E., 2009, The persistence of waterfalls in fractured rock: Geological Society of America Bulletin, v. 121, p. 1123–1134, https://doi.org/10.1130/B26482.1.

Lamb, M.P., and Fonstad, M.A., 2010, Rapid formation of a modern bedrock canyon by a single flood event: Nature Geoscience, v. 3, p. 477–481, https://doi.org/10.1038/ngeo894.

Lamb, M.P., Dietrich, W.E., Aciego, S.M., DePaolo, D.J., and Manga, M., 2008, Formation of Box Canyon, Idaho, by megaflood: Implications for seepage erosion on Earth and Mars: Science, v. 320, p. 1067–1070, https://doi.org/10.1126/science.1156630.

Lamb, M.P., Nittrouer, J.A., Mohrig, D., and Shaw, J., 2012, Backwater and river plume controls on scour upstream of river mouths: Implications for fluvio-deltaic morphodynamics: Journal of Geophysical Research: Earth Surface, v. 117, https://doi.org/10.1029/2011JF002079.

Lamb, M.P., Mackey, B.H., and Farley, K.A., 2014, Amphitheater-headed canyons formed by megaflooding at Malad Gorge, Idaho: Proceedings of the National Academy of Sciences of the United States of America, v. 111, p. 57–62, https://doi.org/10.1073/pnas.1312251111.

Lamb, M.P., Finnegan, N.J., Scheingross, J.S., and Sklar, L.S., 2015, New insights into the mechanics of fluvial bedrock erosion through flume experiments and theory: Geomorphology, v. 244, p. 33–55, https://doi.org/10.1016/j.geomorph.2015.03.003.

Lapotre, M.G.A., Lamb, M.P., and Williams, R.M.E., 2016, Canyon formation constraints on the discharge of catastrophic outburst floods of Earth and Mars: Journal of Geophysical Research: Planets, v. 121, p. 1232–1263, https://doi.org/10.1002/2016JE005061.

Larsen, I.J., and Lamb, M.P., 2016, Progressive incision of the Channeled Scablands by outburst floods: Nature, v. 538, p. 229–232, https://doi.org/10.1038/nature19817.

Larsen, I.J., Farley, K.A., Lamb, M.P., and Pritchard, C.J., 2021, Empirical evidence for cosmogenic $^{3}$He production by muons: Earth and Planetary Science Letters, v. 562, https://doi.org/10.1016/j.epsl.2021.116825.

Lehnigk, K.E., and Larsen, I.J., 2022, Pleistocene megaflood discharge in Grand Coulee, Channeled Scabland, USA: Journal of Geophysical Research: Earth Surface, v. 127, https://doi.org/10.1029/2021JF006135.

Leopold, L.B., Wolman, M.G., and Miller, J.P., 1964, Fluvial Processes in Geomorphology: San Francisco, California, W.H. Freeman & Company, 544 p.

Montgomery, D.R., and Dietrich, W.E., 1989, Source areas, drainage density, and channel initiation: Water Resources Research, v. 25, p. 1907–1918, https://doi.org/10.1029/WR025i008p01907.

Normark, W.R., and Reid, J.A., 2003, Extensive deposits on the Pacific plate from Late Pleistocene North American glacial lake outbursts: The Journal of Geology, v. 111, p. 617–637, https://doi.org/10.1086/378334.

O'Connor, J.E., 1993, Hydrology, Hydraulics and Geomorphology of the Bonneville Flood: Geological Society of America Special Paper 274, 80 p., https://doi.org/10.1130/SPE274-p1.

O'Connor, J.E., and Baker, V.R., 1992, Magnitudes and implications of peak discharges from glacial Lake Missoula: Geological Society of America Bulletin, v. 104, p. 267–279, https://doi.org/10.1130/0016-7606(1992)104<0267:MAIOPD>2.3.CO;2.

O'Connor, J.E., Baker, V.R., Waitt, R.B., Smith, L.N., Cannon, C.M., George, D.L., and Denlinger, R.P., 2020, The Missoula and Bonneville floods—A review of ice-age megafloods in the Columbia River basin: Earth-Science Reviews, v. 208, https://doi.org/10.1016/j.earscirev.2020.103181.

O'Connor, J.E., Clague, J.J., Walder, J.S., Manville, V., and Beebee, R.A., 2022, Outburst Floods, *in* Shroder, J.F., ed., Treatise on Geomorphology (second edition):



Downloaded from http://pubs.geoscienceworld.org/gsa/gsabulletin/article-pdf/136/9-10/4398/6900623/b36975.1.pdf?casa_token=IUGEppbvuJUAAAAA:cP-Iqvj09IGdMOx5aYgrxkIN0Y9yBKjypGEIlcxz3I4RsuNXqhxJW7HKJC
by Univ of Massachusetts Amherst user

Elsevier, p. 765–819, https://doi.org/10.1016/B978-0-12-818234-5.00007-9.

Pardee, J.T., 1942, Unusual currents in glacial Lake Missoula, Montana: Geological Society of America Bulletin, v. 53, p. 1569–1600, https://doi.org/10.1130/GSAB-53-1569.

Pico, T., David, S.R., Larsen, I.J., Mix, A., Lehnigk, K., and Lamb, M.P., 2022, Glacial isostatic adjustment directed incision of the Channeled Scabland by ice-age megafloods: Proceedings of the National Academy of Sciences, v. 119, https://doi.org/10.1073/pnas.2109502119.

Playfair, J., 1802, Illustrations of the Huttonian Theory of the Earth: London, Cadell and Davies, 528 p.

Praetorius, S.K., Condron, A., Mix, A.C., Walczak, M.H., McKay, J.L., and Du, J., 2020, The role of Northeast Pacific meltwater events in deglacial climate change: Science Advances, v. 6, https://doi.org/10.1126/sciadv.aay2915.

Reidel, S.P., and Tolan, T.L., 2013, The Grande Ronde Basalt, Columbia River Basalt Group, *in* Reidel, S.P., Camp, V.E., Ross, M.E., Wolff, J.A., Martin, B.S., Tolan, T.L., and Wells, R.E., eds., The Columbia River Flood Basalt Province: Geological Society of America Special Paper 497, p. 117–153, https://doi.org/10.1130/2013.2497(05).

Roberts, S.G., Nielsen, O., Gray, D., Sexton, J., and Davies, G., 2015, ANUGA User Manual Release 2.0, https://doi.org/10.13140/RG.2.2.12401.996.

Savitzky, A., and Golay, M.J.E., 1964, Smoothing and differentiation of data by simplified least squares procedures: Analytical Chemistry, v. 36, p. 1627–1639.

Schwanghart, W., and Scherler, D., 2014, TopoToolbox 2—MATLAB-based software for topographic analysis and modeling in Earth surface sciences: Earth Surface Dynamics, v. 2, p. 1–7, https://doi.org/10.5194/esurf-2-1-2014.

Seidl, M.A., and Dietrich, W.E., 1992, The problem of channel erosion into bedrock, *in* Schmidt, K.H., and de Ploey, J., eds., Functional Geomorphology: Cremlingen-Destedt, Germany, Catena Verlag, v. 23, p. 101–124.

Smith, L.N., 2006, Stratigraphic evidence for multiple drainings of glacial Lake Missoula along the Clark Fork River, Montana, USA: Quaternary Research, v. 66, p. 311–322, https://doi.org/10.1016/j.yqres.2006.05.009.

Swanson, D.A., and Wright, T.L., 1978, Bedrock geology of the northern Columbia Plateau and adjacent areas, *in* Baker, V.R., and Nummedal, D., eds., The Channeled Scabland: A Guide to the Geomorphology of the Columbia Basin, Washington: U.S. National Aeronautics and Space Administration, Comparative Planetary Geology Field Conference, Columbia Basin, Washington, USA, 5–8 June, p. 37–57.

USDA-NRCS-NCGC (US Department of Agriculture Natural Resources Conservation Service National Cartography and Geospatial Center), 2009, Digital Ortho Mosaic: USDA/NRCS–National Geospatial Center of Excellence, https://datagateway.nrcs.usda.gov/GDGHome_DirectDownLoad.aspx.

Valla, P.G., Van der Beek, P.A., and Lague, D., 2010, Fluvial incision into bedrock: Insights from morphometric analysis and numerical modeling of gorges incising glacial hanging valleys (Western Alps, France): Earth and Planetary Science Letters, v. 104, p. 424–439.

Wahba, G., 1990, Spline Models for Observational Data: Philadelphia, Society for Industrial and Applied Mathematics, 169 p., https://doi.org/10.1137/1.9781611970128.

Waitt, R.B., 1980, About forty last-glacial Lake Missoula jökulhlaups through southern Washington: The Journal of Geology, v. 88, p. 653–679, https://doi.org/10.1086/628553.

Waitt, R.B., 1985, Case for periodic, colossal jökulhlaups from Pleistocene glacial Lake Missoula: Geological Society of America Bulletin, v. 96, p. 1271–1286, https://doi.org/10.1130/0016-7606(1985)96<1271:CFPCJF>2.0.CO;2.

Waitt, R.B., 2002, Great Holocene floods along Jökulsá á Fjöllum, north Iceland, *in* Martini, I.P., Baker, V.R., and Garzón, G., eds., Flood and Megaflood Processes and Deposits: Recent and Ancient Examples: New York, Wiley, International Association of Sedimentologists, p. 37–51, https://doi.org/10.1002/9781444304299.ch3.

Waitt, R.B., 2016, Megafloods and Clovis cache at Wenatchee, Washington: Quaternary Research, v. 85, p. 430–444, https://doi.org/10.1016/j.yqres.2016.02.007.

Waitt, R.B., 2021, Roads less travelled by—Pleistocene piracy in Washington's northwestern Channeled Scabland, *in* Waitt, R.B., Thackray, G.D., and Gillespie, A.R., eds., Untangling the Quaternary Period—A Legacy of Stephen C. Porter: Geological Society of America Special Paper 548, p. 351–384, https://doi.org/10.1130/2021.2548(18).

Waitt, R.B., and Atwater, B.F., 1989, Stratigraphic and geomorphic evidence for dozens of last-glacial floods, *in* Breckenridge, R.M., Atwater, B.F., Baker, V.R., Busacca, A.J., Chambers, R.L., Curry, R.R., Hanson, L.G., Kever, E.P., McDonald, E.V., Stradling, D.F., and Waitt, R.B., Jr., eds., Glacial Lake Missoula and the Channeled Scabland Missoula, Montana to Portland, Oregon, July 20–26, 1989: Washington, D.C., American Geophysical Union, p. 37–50, https://doi.org/10.1029/FT310p0037.

Waitt, R.B., O'Connor, J.E., and Harpel, C.J., 2000, Varying routings of repeated colossal jökulhlaups through the channeled scabland of Washington, USA: Orkustofnun Rept. OS-2000/036, Reykjavık, Extremes of the Extremes Conference, v. 27.

Waitt, R.B., Atwater, B.F., Hanson, M.A., Lehnigk, K.E., Larsen, I.J., Bjornstad, B.N., and O'Connor, J.E., 2021, Upper Grand Coulee: New views of a channeled scabland megafloods Enigma, *in* Booth, A.M., and Grunder, A.L., eds., From Terranes to Terrains: Geologic Field Guides on the Construction and Destruction of the Pacific Northwest: Geological Society of America Field Guide 62, p. 245–300, https://doi.org/10.1130/2021.0062(07).

Washington State Department of Natural Resources, 2010, Digital Geology of Washington State, version 3.0: Division of Geology and Earth Resources GIS data, 1:100,000 scale, https://www.dnr.wa.gov/programs-and-services/geology/publications-and-data/gis-data-and-databases.

Whipple, K.X., and Tucker, G.E., 1999, Dynamics of the stream-power river incision model: Implications for height limits of mountain ranges, landscape response timescales, and research needs: Journal of Geophysical Research: Solid Earth, v. 104, p. 17,661–17,674, https://doi.org/10.1029/1999JB900120.

Wobus, C., Whipple, K.X., Kirby, E., Snyder, N., Johnson, J., Spyropolou, K., Crosby, B., and Sheehan, D., 2006, Tectonics from topography: Procedures, promise, and pitfalls, *in* Willett, S.D., Hovius, N., Brandon, M.T., and Fisher, D.M., eds., Tectonics, Climate, and Landscape Evolution: Geological Society of America Special Paper 398, Penrose Conference Series, p. 55–74, https://doi.org/10.1130/2006.2398(04).

Science Editor: Brad Singer
Associate Editor: Alexander Whittaker

Manuscript Received 9 February 2023
Revised Manuscript Received 23 January 2024
Manuscript Accepted 29 February 2024



Downloaded from http://pubs.geoscienceworld.org/gsa/gsabulletin/article-pdf/136/9-10/4398/6900623/b36975.1.pdf?casa_token=IUGEppbvuJUAAAAA:cP-Iqvj09IGdMOx5aYgrxkIN0Y9yBKjypGEIlcxz3I4RsuNXqhxJW7HKJC
by Univ of Massachusetts Amherst user